LAWRENCE
LIVERMORE
NATIONAL
LABORATORY

LLNL-JRNL-791483

Measurement of PuO2 Film Thickness by Electron Probe Microanalysis (EPMA) calibration curve method

J. A. Stanford, N. Teslich, S, Donald, C. K. Saw, R. Gollott, L. N. Dinh

September 26, 2019

Journal of Nuclear Materials

Disclaimer

This document was prepared as an account of work sponsored by an agency of the United States government. Neither the United States government nor Lawrence Livermore National Security, LLC, nor any of their employees makes any warranty, expressed or implied, or assumes any legal liability or responsibility for the accuracy, completeness, or usefulness of any information, apparatus, product, or process disclosed, or represents that its use would not infringe privately owned rights. Reference herein to any specific commercial product, process, or service by trade name, trademark, manufacturer, or otherwise does not necessarily constitute or imply its endorsement, recommendation, or favoring by the United States government or Lawrence Livermore National Security, LLC. The views and opinions of authors expressed herein do not necessarily state or reflect those of the United States government or Lawrence Livermore National Security, LLC, and shall not be used for advertising or product endorsement purposes.

LLNL-JRNL-791483

Measurement of PuO_2 Film Thickness by Electron Probe Microanalysis (EPMA) calibration curve method

J. A. Stanford, N. Teslich, S. Donald, C. K. Saw, R. Gollott, and L. N. Dinh*

AFFILIATIONS
Lawrence Livermore National Laboratory, Livermore, California 94551, USA
* Contacting author: dinh1@llnl.gov, 1-925-422-4271

ABSTRACT

Plutonium (Pu) surfaces are highly reactive toward oxygen containing species and, therefore, invariably covered with oxides (e.g. PuO_2) during transport and handling. The actual thickness of the surface oxide may dictate if a plutonium part is suitable for a certain application. As a result, a cost-effective, quick, non-destructive, yet reliable means to measure the oxide layer thickness formed on Pu samples is desirable. In this study, the cross-sections of a series of room temperature grown oxides on Pu samples were trenched by focus ion beam (FIB) then observed by scanning electron microscopy (SEM) to measure the surface oxide thicknesses, which were then combined with the corresponding oxygen k-ratios provided by electron probe microanalysis (EPMA) to form calibration curves. Oxide thickness measurements for the calibration curves were made on samples within the typical SEM observable range for PuO_2 (35 – 400 nm). The portion of the calibration curve in the thinner oxide region (< 35 nm) were approximated via Pouchou and Pichoir's $\varphi(\rho z)$ theory. Two specimens with micrometer-thick PuO_2 standards (one formed at room temperature and the other at higher temperature with a higher level of crystallinity) were made for the k-ratios in this study, allowing EPMA users to choose the standard that best suits their needs. If the surface corrosion is known to be PuO_2 (from the environment in which the Pu sample is stored) or if the stoichiometry of the surface oxide is

confirmed by a preliminary/compliment technique, these calibration curves allow EPMA users to quickly and efficiently determine PuO_2 thicknesses from the measured oxygen k-ratios of their samples. The methodology presented in this study can also be used as a template for creating calibration curves for oxides grown on other actinides.

1. INTRODUCTION

In dry air, a thin protective layer of PuO_2 quickly forms on bare alpha phase plutonium metal, like iron and restricts the oxidation rate to 20 picometers per hour [1,2]. The oxide layer eventually reaches a stable thickness of 4 -5 micrometers [1,2]. Moisture and heat are factors that can greatly increase the oxidation rate [1,2]. However, the oxidation reaction rate is reduced when plutonium is alloyed with gallium (delta-phase gallium-stabilized alloy) [1-3]. The plutonium oxidation rate is, indeed, a complex function of alloy type/fraction, oxidizing species (air, oxygen, moisture, etc.), concentration, and temperature.

Because of these varying oxidation rates, there is a need to measure and control the oxide thicknesses on Pu parts for suitability with intended applications. Technical issues pose challenges to several instrumentational methods that have been used to measure plutonium oxide thicknesses. Depth profiling with Auger electron spectroscopy (AES) or x-ray photoelectron spectroscopy (XPS) requires sputtering rates, which can only be determined by combining AES/XPS results at each sputtered depth with profilometry or by *sputter-rate standards* – both techniques are time consuming and technically challenging for plutonium [4]. The X-ray reflectivity technique (XRR) can be used for thickness measurements, however, the surface roughness of the plutonium metal can adversely affect the spectra quality and the technique is

optimal for thicknesses less than 50 nm [5]. A SEM instrument, equipped with a focused ion beam (FIB) could mill micrometer scale trenches out of a sample to measure the oxide films, however, this method is destructive to the analysis area [6]. Extensive sample preparation and lengthy data acquisition time are challenges for thin film measurement by transmission electron microscopy (TEM). Ellipsometry is very sensitive to surface roughness and may yield non-unique results unless combined with another complementary technique if the optical constants for the substrate and the oxide layer are not known ahead of time [7]. The JEOL Thin Film Analysis software for the EPMA will only quantify thin film samples that do not have a common element in the base metal and the thin film [8,9]. Other methods of EPMA thin film measurement schemes include mathematically based software programs, Monte Carlo simulations, and the calibration curve method [10]. Various EPMA methodologies have been successfully employed to extract thicknesses of oxides grown on metals [11-14]. However, at the present time, there is only one publication describing measurement results for plutonium oxide films using an EPMA combined with STRATAGem software which implements an expanded version of Pouchou and Pichoir's model of $\varphi(\rho z)$ theory [2,15]. In that study, STRATAGem's k-ratio versus voltage computation function estimated PuO_2 layer thicknesses (grown under ambient conditions) with no independent means of verifying the thickness estimates [2]. In addition, the crystalline structure of PuO_2 grown at low temperature has an amorphous fraction which leads to an unpredictable density value, preventing the use of STRATAGem alone as a reliable tool for accurate PuO_2 thickness calculations without another complementary experimental technique [16].

Because of the complexity and limitation of the mentioned approaches, an economical, fast, non-destructive, and dependable method to measure the oxide layer formed on Pu samples is highly desirable. Such an approach can be the calibration curve method with EPMA to obtain the oxygen k-ratios in the oxides and a complementary technique to measure the oxide thicknesses [10]. By plotting thickness measurements against k-ratios, an analyst can create a "working curve" which can be used to predict film thicknesses by referencing EPMA k-ratios [10]. At the present time, no systematic study has been performed on plutonium oxide films using the EPMA calibration curve method. In this paper, EPMA oxygen k-ratios were experimentally obtained at accelerating voltages of 10 and 12 keV from a set of PuO_2 films grown at room temperature on plutonium substrates. The oxide thicknesses were measured by SEM observation of cross-sections trenched by a FIB. The characteristic X-ray intensities of the PuO_2 thin films were ratioed with the intensity of PuO_2 standards to create the k-ratios. The measured oxide thicknesses varied from 35 – 403 nm. Pouchou and Pichoir's (PAP) model for parabolic representation of $\varphi(\rho z)$ distribution was utilized to project the calibration curves thicknesses downward for thicknesses less than 35 nm [17]. The obtained calibration curves allow EPMA analysts to quickly, economically, and effectively determine the thickness of a PuO_2 layer on plutonium metal using the oxygen k-ratio intensities. This study applies the calibration curve method for oxide thin film thickness determination [11-14] to nuclear materials.

2. MATERIALS AND METHODS

2.1. Material Preparation

CASINO, a software program designed to predict electron trajectories by Monte Carlo simulation, was used to assess the range of electron penetration depth in PuO_2 layers [18]. Based on CASINO simulations, PuO_2 thickness grown for the microprobe standards were

recommended to be > 1μm to encapsulate the full range of electron penetration in the range of 10 to 12 keV.

Initial lapping of all Pu samples and standards consisted of a series of USA standard abrasive size SiC disks (240, 320, 400, 600, and 600 soft) followed by 9 μm and 5 μm Al_2O_3 lapping film. The Pu samples and standards were then hand-polished with 1 μm diamond paste in kerosene on microCloth to prepare clean and relatively smooth surfaces for subsequent oxide growth. Two samples with micrometer-thick PuO_2 films grown on delta Pu (δ-Pu) with 0.5 wt.% gallium (Ga) were used as the EPMA standards for this study. The oxide on one EPMA standard was created at 50 kPa of dry air (ppm moisture) at 425 °C for 3 – 4 hours, forming the high temperature EPMA standard in this report. The oxide on the other EPMA standard was grown at low temperature (~ 27 °C) with low air pressure (67 – 80 kPa) for ~ three months, forming the low temperature standard. The series of samples employed to obtain the calibration curves in this report have ~ 35 nm to 400 nm oxide thicknesses, formed by exposure to air at low temperature from a few hours to a few months. After EPMA, a FIB was used to mill cross-sectional trenches at site specific locations on this series of samples, then a SEM with a FEI Quanta 3D Field Emission Gun (FEG) was employed to measure the oxide thicknesses of the samples. An example of a PuO_2 cross-section imaged by the FEI Quanta 3D FEG/FIB SEM is displayed in Figure 1. The sample oxygen X-ray EPMA intensities, ratioed with the oxygen standard EPMA intensity values, generated k-ratio ($I_{UNKNOWN}/I_{STANDARD}$) values. K-ratios were gathered at ten fiduciary locations on the samples followed by ten corresponding oxide measurement trenches at these same locations, providing ten data points for the calibration curves. The k-ratios were used

to create four calibration curves using the low temperature and high temperature standard at 10 and 12 keV.

2.2. Philips vertical goniometer x-ray diffractometer operation

A Philips vertical goniometer x-ray diffractometer was used to evaluate the crystalline structure of the two standards using a copper Kα source (8.04 keV) with Bragg-Brentano geometry. The diffractometer step scan ranged from 20º to 80º (θ) with 0.02° per step with 4 seconds dwell time. A thin piece of Kapton film covered the standards for contamination control.

2.3. EPMA Operation

A JEOL 8230 Superprobe EPMA acquired oxygen Kα x-ray intensities for the standards and the samples at accelerating voltages of 10 and 12 keV with a constant amperage of 30 nA. The on-peak EPMA count time was 20 seconds while the upper and lower background count times were 10 seconds. A normal type wavelength dispersive spectrometer, using a LDE2 diffraction crystal (~ 10 nm 2*d* spacing) with a *P*-10 gas flow-proportional x-ray detector, collected the oxygen Kα x-ray line data. The EPMA take-off angle, which is the angle formed between the plane of the sample and the detector, was 40°. For each sample thickness and keV setting, the EPMA was programmed to analyze ten standard spots for the average intensity, which was then divided by the value from the oxide standard to produce the corresponding k-ratio. The JEOL EMPA software applied background subtraction to the final k-ratios via the spectrometer displacement method where the X-ray intensity from the upper and lower background positions are averaged and subtracted from the gross oxygen Kα x-ray intensities [19].

2.4. Quanta 3D FEG/FIB Operational Parameters

For each sample, only one trench with 2 μm along the x-axis, 9 μm along the y-axis, and 3 μm in depth along the z-axis was created near the vicinity of the location where EPMA were previously performed. From these trends, many cross-sectional SEM images were measured to obtain average oxide thicknesses and associated error bars for the samples. The nanoscale cross-section can then be viewed via SEM column. Table 1 describes the voltage and amperage parameters for the various operations to trench and observe the oxide layer cross-section.

Table 1 – Voltage and amperage parameters for operations to trench and observe the oxide layer cross-section.

Operation	Voltage	Amperage
Electron beam deposition	2 keV	24 nA
Ion beam deposition	30 keV	0.3 nA
Trench milling	30 keV	1.0 nA
Cleaning cross-section	30 keV	0.1 nA
SEM imaging	10 keV	0.19 nA

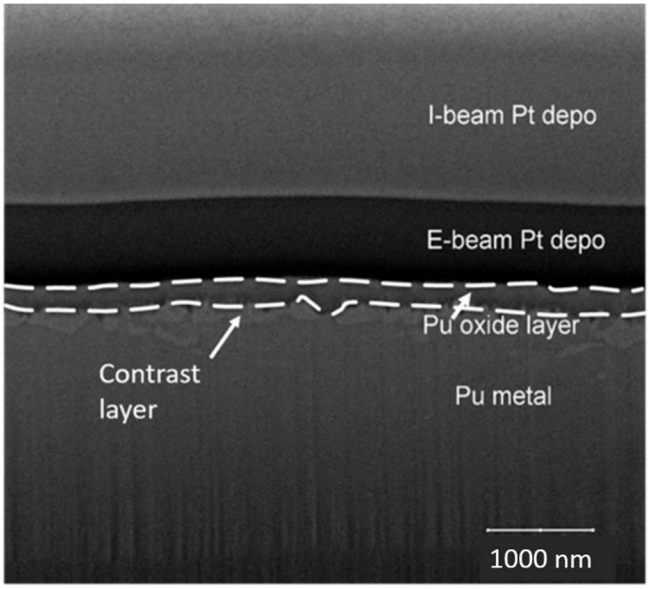

Fig. 1: A cross-sectional view of a PuO_2 layer on a sample by the FEI Quanta 3D FEG/FIB SEM.

2.5. AES Operation

Auger electron spectroscopy experiments were carried out using a PHI 710 scanning Auger nanoprobe equipped with a field-emission electron gun and co-axial cylindrical mirror analyzer (CMA), possessing an energy resolution of $\Delta E/E = 0.5\%$ housed in an ultra-high vacuum chamber with a base pressure of 2×10^{-10} Torr. Line scan analyses were acquired with an incident electron beam at 20 keV and 1 nA, which produced an electron beam of ~30 nm in diameter. Quantitative compositional analysis using Auger peak-to-peak heights and linear least squares fitting was obtained from the Auger peak intensities and line-shapes for each element present using MultiPak 9.6 (PHI) [20].

2.6. Extrapolation of calibration curves at very thin and very thick PuO_2 limits

The $\varphi(\rho z)$ distribution is an expression of the x-ray intensity as a function of depth or mass depth (ρz is *density* • *depth*) and usually expressed in the unit of g/cm^2 [21]. The entire distribution of a $\varphi(\rho z)$ curve represents the full amount of x-ray radiation emitted by a given element. Only a fraction of the low end of the $\varphi(\rho z)$ graph represents the x-ray intensity from an element in a thin film. Accordingly, a sufficient approximation of a k-ratio versus depth distribution is proportional to $\int_0^{\rho z} \varphi(\rho z)\, d(\rho z)$, implying a higher k-ratio for thicker oxide film. In an actual k-ratio measurement, the thin film x-ray intensity is divided by the full intensity of the distribution provided by the standard, which is a constant. The PAP procedure for $\varphi(\rho z)$ distributions was applied to estimate the lower end of the calibration curves past the lowest experimentally

acquired oxide thickness [17]. According to the PAP model, the φ(ρz) distribution for a film on a substrate can be represented by two successive parabolas with equal magnitude and slope at a mass depth value of R_c as qualitatively illustrated in Fig. 2 [17].

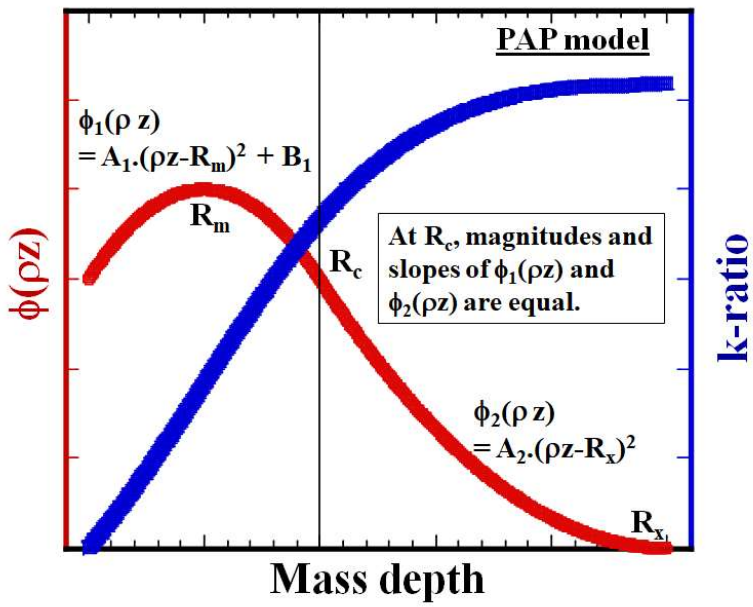

Fig. 2: A qualitative illustration of the PAP model (with A_1 = -1, A_2 = 1/3, B_1 = 400, R_m = 10, R_c = 20, and R_x = 50). The red graph represents the φ(ρz) curve. The blue graph is the integral of the φ(ρz) curve representing, the k-ratio approximation.

The requirements for equal magnitude and slope at the location where the first parabola meets the second parabola (R_c) can be written mathematically as following:

Equal magnitude:

$$A_1 (R_c - R_m)^2 + B_1 = A_2(R_c - R_x)^2 \quad (1)$$

Equal slope:

$$A_1 (R_c - R_m) = A_2(R_c - R_x) \quad (2)$$

In Fig. 2, R_m and R_x stand for the mass depth values at the peak of the first parabola, $\phi_1(\rho z)$, where the oxygen X-ray intensity is highest and at the bottom of the second parabola, $\phi_2(\rho z)$,

which represents the maximum oxide thickness beyond which oxygen X-ray intensity diminishes to zero, respectively. Currently, there is no available information on A_1, A_2, B_1, R_m, R_c, and R_x to build a quantitative PAP model for PuO_2 films grown on Pu. Fig. 2 is presented here for readers to visualize the qualitative connection between $\phi(\rho z)$ and oxygen k-ratio which is proportional to the area under the $\phi(\rho z)$ curve. From Fig. 2, the portion of the oxygen k-ratio from 0 to R_c is proportional to the area under the first parabola $\phi_1(\rho z)$ and can be mathematically described by a third degree polynomial going through the origin (of the form $y_1 = a_1x^3 + b_1x^2 + c_1x$) so that the oxygen k-ratio is equal to zero when the oxide thickness is zero. The portion of the oxygen k-ratio from R_c to R_x is proportional to the summation of the total area under the $\phi_1(\rho z)$ curve from 0 to R_c (a constant positive value) and the area under the $\phi_2(\rho z)$ curve, and therefore should be mathematically described by another third degree polynomial which does not go through the origin (of the form $y_2 = a_2x^3 + b_2x^2 + c_2x + d_2$).

Hence the calibration curves were extended downward for oxide thicknesses thinner than the FEI Quanta 3D FEG/FIB instrument's resolution capability (around 35 nm) by means of a third-degree polynomial mathematical fit of the form $y_1 = a_1x^3 + b_1x^2 + c_1x$ to the experimental data. As the oxide film gets very thick (greater than 400 nm), the collected oxygen x-ray intensity approaches a saturation limit and increases very little with the oxide thickness. This portion of the calibration curves represents the gradual asymptotic increase of k-ratio values towards 1.0 as the oxide thicknesses increases and should be well modeled by a third-degree polynomial of the form $y_2 = a_2x^3 + b_2x^2 + c_2x + d_2$.

3. RESULTS AND DISCUSSION

3.1. The dependence of oxide crystallinity on synthesis temperature

The 9 µm and 1.2 µm measured for the oxides on the high and low temperature PuO_2 standards provided adequate oxide thickness to encapsulate the interaction volume for both 10 and 12 keV EPMA settings. The two standard oxide layers were further examined by x-ray diffraction as displayed in Fig. 3.

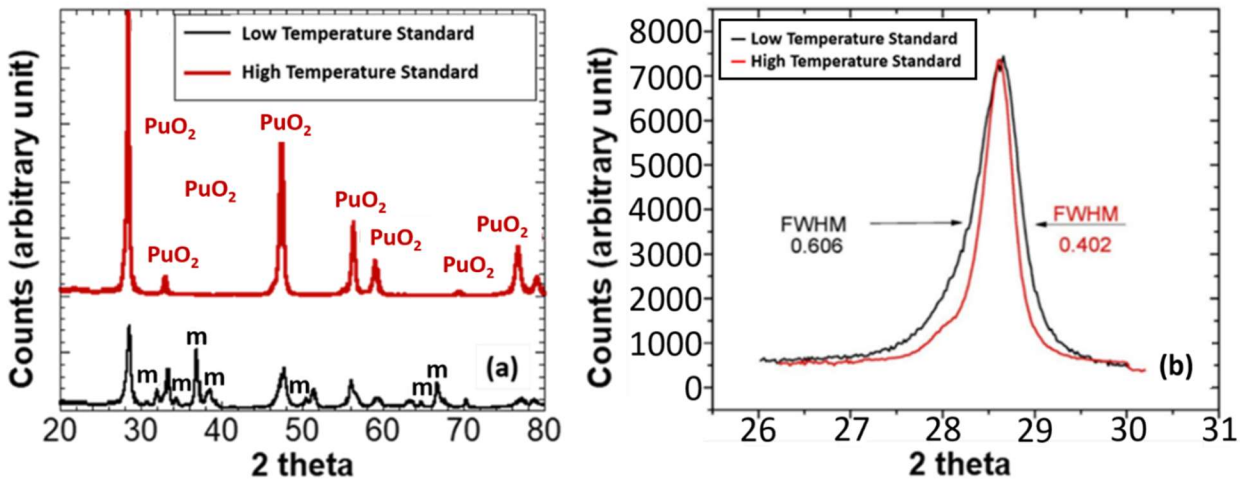

Fig. 3: (a) X-ray diffraction results of the high temperature and low temperature standards. The peaks from the metal below the Pu oxide layer are annotated with "m".; (b) The oxide peak profiles from the (111) plane for the same two standards.

The high temperature standard has superior crystallinity compared to the low temperature standard as demonstrated by the narrower Full Width Half Maximum (FWHM) of the X-ray Diffraction (XRD) peaks in Fig. 3(a). As indicated in Fig. 3(b), the major (111) peak from the oxide phase of the high temperature standard has a smaller full width at half maximum compared to the low temperature standard (0.402 compared to 0.606 FWHM, respectively). Considering the Scherrer equation, which states the crystallite size or crystallite order is inversely proportional to the measured FWHM of the XRD peak minus the instrument broadening, the narrower FWHM indicates a larger crystallite size. Higher temperature synthesis provides the extra

energy necessary to move the atoms into the more favorable thermodynamic position in the material network and to reduce the internal energy of the growing films by reducing the total area of grain boundary, resulting in larger and more perfect crystals. In addition, at lower temperature settings, the atoms do not have the necessary kinetic energy to arrange themselves into more orderly formation, resulting in a certain fraction of amorphous structure. The reduced density of the low temperature standard with an amorphous fraction (compared to the high temperature standard) results in a reduced overall oxygen X-ray intensity from the EPMA. The XRD peaks from the Pu metal below the 1.2 μm Pu oxide layer are present in the diffraction pattern of the low temperature standard and are labeled "m" in Fig. 3a.

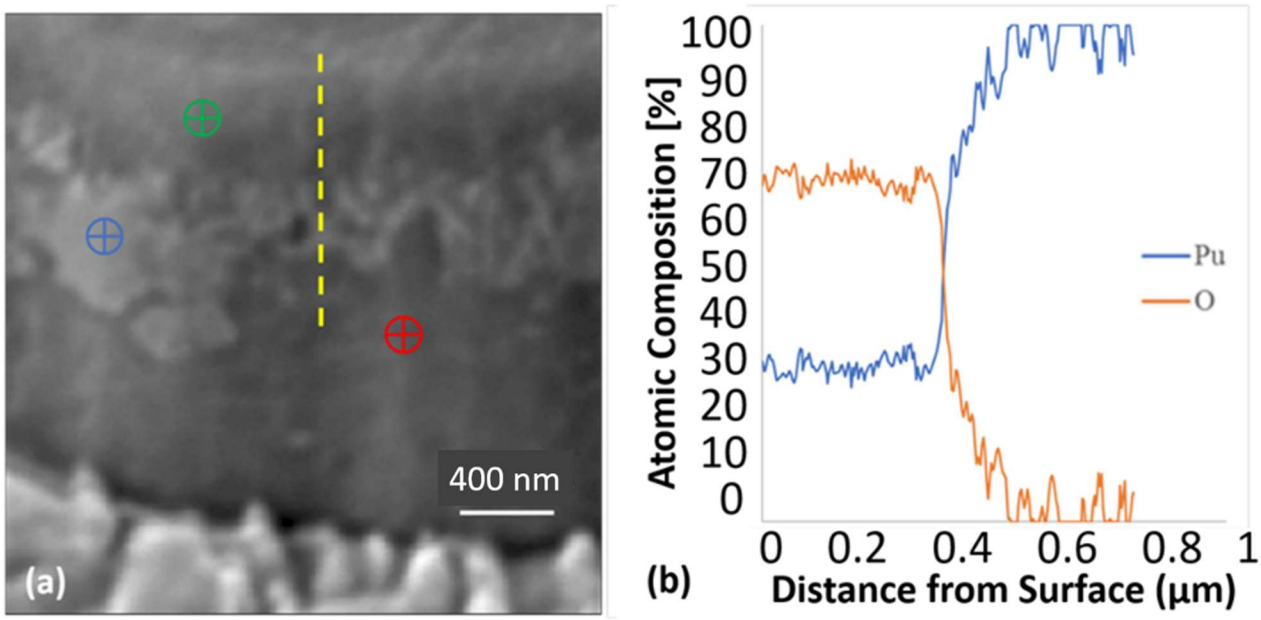

Fig. 4: (a) A cross-sectional view of a PuO_2 layer from a sample by the PHI 701 SAN. The green target is located on the Pu oxide layer, the blue target is located on the brighter contrast area, and the red target is located on the Pu metal substrate; (b) AES line scan analysis taken across the cross-section indicates the oxide is relatively uniform in composition, with an overall stoichiometry of PuO_2.

3.2. Contrast Layer

As shown in Figures 1 and 4, a distinct layer of increased brightness was observed below the PuO_2 layer in all SEM cross-sections of the samples and the oxide standards. Line and point scan AES analyses performed along the cross-section (as shown in Figure 4) indicated this area to be metallic plutonium with similar chemical composition to the bulk sample, as shown in Table 2. The contrast in this layer indicates a change in the secondary electron yield and may be the result of differences in density or lattice orientation as opposed to chemical composition. The AES nanoprobe was out of alignment during the time of image acquisition for Fig. 4a which caused poor image quality and the sample couldn't be reintroduced back into the instrument after the alignment was performed. In addition, it is noted that AES probing depth is very shallow (2 to 3 nm) and the 1 to 4% carbon listed in Table 2 indicates that the detected carbon was just accidental contamination during operation and is much less than one monolayer coverage. There was no observable charging (conformance to Duane-Hunt limit) and no carbon or any conductive coating was needed for the samples in this work.

Table 2 – AES composition analysis of cross-section regions in atomic percentage.

Location	C	O	Pu	O:Pu
Oxide (Green)	1.05	65.78	33.17	1.98
Bright Metal (Blue)	4.32	10.09	85.60	0.12
Dark Metal (Red)	4.53	11.27	84.20	0.13

3.3. Calibration curves for quick determination of PuO_2 thickness via EPMA

Table 3 – Summary of experimentally gathered data for calibration curves

Oxide thickness	Oxygen k-ratio (normalized with high temperature standard)		Oxygen k-ratio (normalized with low temperature standard)	
(nm)	10 keV k-ratio	12 keV k-ratio	10 keV k-ratio	12 keV k-ratio
34.8	0.1712	0.1457	0.1653	0.1435
56.8	0.2367	0.1744	0.2512	0.1880
78.6	0.3303	0.3110	0.3705	0.3267
90.4	0.4201	0.3745	0.3902	0.3654
118.3	0.5822	0.4772	0.6022	0.5279
138.7	0.6619	0.5820	0.6660	0.5934
248.5	0.8301	0.8174	0.8874	0.8854
309.0	0.8713	0.8217	0.9176	0.8902
335.0	0.9376	0.9214	0.9683	1.0208
403.4	0.9575	0.9647	0.9764	0.9942

Table 3 summarizes the experimental data for the calibration curves at 10 keV and 12 keV. The oxide thickness column was obtained by FIB trenching followed by cross-section SEM observation. The oxygen k-ratio columns were the result of dividing the EPMA measured oxygen x-ray intensity of each sample by the measured x-ray intensities of the high and low temperature oxide standards. From Table 3, it is observed that the spread in the oxygen k-ratio for oxide films from 34.8 nm to 403.4 nm is larger at 12 keV setting than at 10 keV setting. So, lowering the electron accelerating voltage to below 10 keV would cover a smaller oxide thickness range with an increased resolution, while increasing the electron accelerating voltage to higher than 12 keV would cover a larger range of the oxide thickness with a reduced resolution. The 10 keV and 12 keV settings in this work were chosen to adequately cover the practical oxide range of 0 nm to 400 nm. Other electron accelerating voltages for EPMA operation can also be tailored for different oxide ranges with thinner/thicker maximum oxide thickness.

The calibration curves which convert measured EPMA oxygen k-ratios into corresponding oxide thicknesses with the 10 keV setting and the 12 keV setting are shown in Figs. 5 and 6, respectively. The 10 data points in Figs. 5 & 6 were from 10 test samples with different oxide thicknesses grown on plutonium substrate at room temperature. The k-ratio for each of the data point was obtained by dividing the oxygen x-ray intensity for that film by the oxygen x-ray intensity from either the low temperature oxide standard (Figs. 5(a) and 6(a)) or the high temperature oxide standard (Figs. 5(b) and 6(b)). The corresponding oxide thickness for each data points were extracted from FIB trenching followed by observation of the cross-section with SEM as described in the "Materials and Methods" section. In Figs. 5 & 6, the calibration curves were extended downward for oxide thicknesses thinner than 35 nm by means of a third-degree polynomial mathematical fit (going through the origin) to the experimental data up to ~ 200 nm as explained in the "Materials and Methods" section (see ***"2.6. Extrapolation of calibration curves at very thin and very thick PuO_2 limits"***). However, without losing much accuracy, the downward extension to below 35 nm can practically be done by a linear fit since the linear term in a third-degree polynomial fit dominates the curve at smallest values of oxide thicknesses. The data near the thicker oxide region (200 nm to 400 nm) were well fitted to a third-degree polynomial which does not go through the origin as discussed in the "Materials and Methods" section (see ***"2.6. Extrapolation of calibration curves at very thin and very thick PuO_2 limits"***). Within the magnitude of the error bars associated with the data used in the calibration curves, the region of the calibration curves between 140 nm and 200 nm can be approximated by either of the two third degree polynomial fits. Fig. 5 can be used to calculate oxide thicknesses at the 10 keV setting using the low temperature or the high temperature standard. Fig. 6 can be used to

calculate oxide thicknesses at the 12 keV setting using the low temperature or high temperature standard. The error bars displayed in Figs. 5 & 6 correspond to one sigma standard deviation.

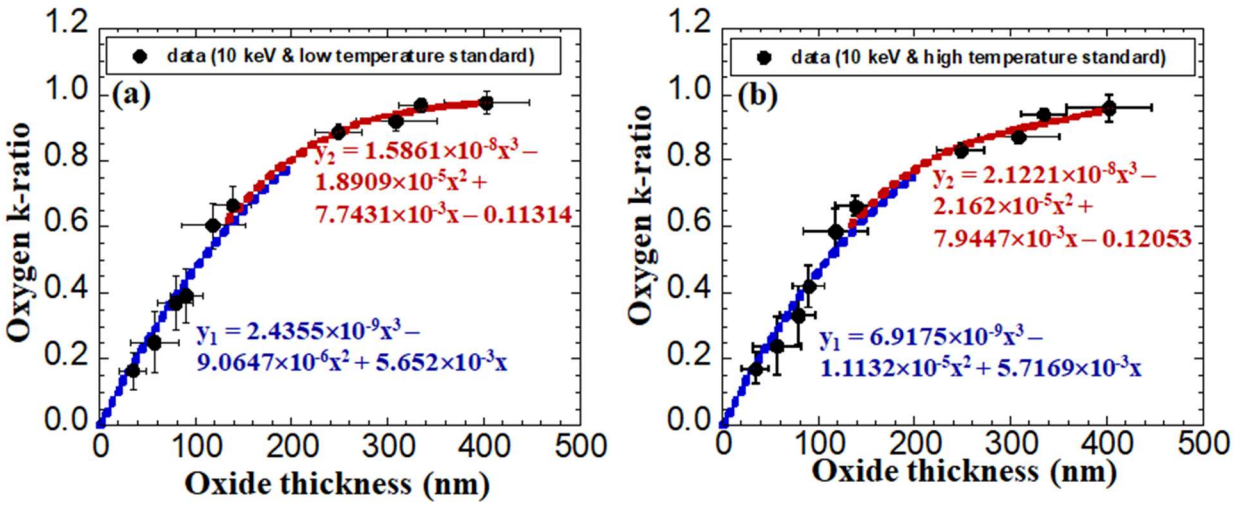

Fig. 5 - The calibration curves to convert from EPMA oxygen k-ratios into oxide thicknesses at 10 keV for the (a) low temperature oxide standard and (b) high temperature oxide standard. A third-degree polynomial fit running through the origin was applied to the thinner oxide region. Another third-degree polynomial fit (not going through the origin) was applied to thicker oxide region.

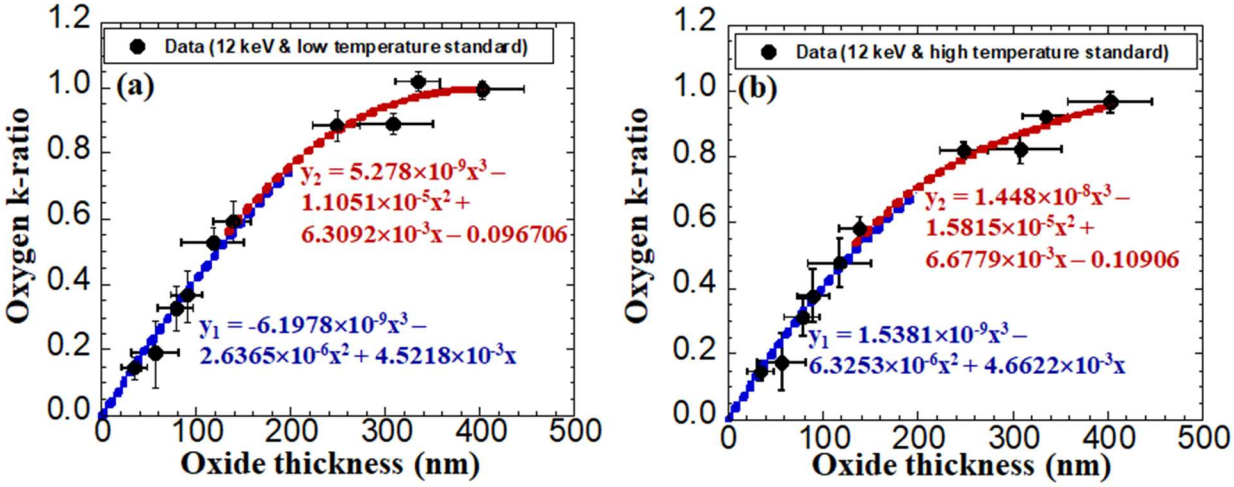

Fig. 6 - The calibration curves to convert from EPMA oxygen k-ratios into oxide thicknesses at 12 keV for the (a) low temperature oxide standard and (b) high temperature standard. A third-degree polynomial fit running through the origin was applied to the thinner oxide region. Another third-degree polynomial fit (not going through the origin) was applied to thicker oxide region.

To use the calibration curves to determine an oxide thickness in the range of 0 – 400 nanometers, EPMA users must first grow a sufficiently thick oxide layer (significantly greater than 400 nm) to be used as PuO_2 standard. The user will then acquire oxygen intensities from both the sample and the PuO_2 standard to obtain the oxygen k-ratio value as described in the *EPMA Operation* section. To fully integrate the use of the calibration curves presented in Figs. 5 & 6, one must first ensure that the surface corrosion layer is PuO_2. The users can either use the provided calibration curves or employ the polynomial fits provided in Figs. 5 & 6 to read out the oxide thickness of the sample. The purpose of these calibration curves is to give a correlation between the k-ratio and the oxide thickness. If the oxide layer thickness varies significantly, then the researcher needs to collect k-ratios at several appropriate locations, then use the calibration curves to obtain the variation in oxide thickness.

From XRD results (Fig. 3), the high temperature standard is more crystalline and so is expected to have a higher density value than the low temperature standard synthesized at room temperature. However, the density values of the low and high temperature standards are not known. From Table 3, by dividing the values in column 4 (oxygen k-ratios with the low temperature standard at 10 keV) by those in column 2 (oxygen k-ratios with the high temperature standard at 10 keV), the ratios of the oxygen x-ray intensities for the low and high temperature standards at 10 keV for all the examined oxide thicknesses can be obtained. Similarly, by dividing the values in column 5 by those in column 3, the ratios of the oxygen x-ray intensities for the low and high temperature standards at 12 keV for all tested samples can be extracted. The results are plotted in Fig. 7.

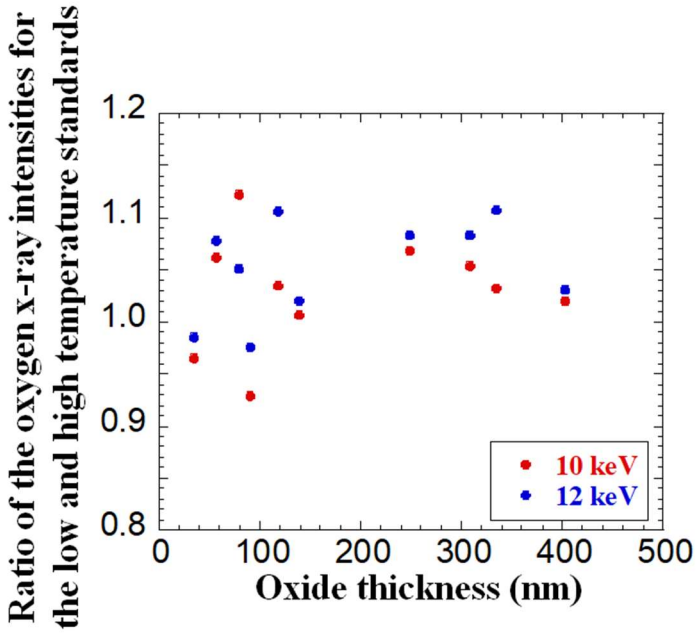

Fig. 7: The ratio of the oxygen x-ray intensities for the low and high temperature standards vs. oxide thickness from Table 3.

Theoretically, the ratio of the oxygen x-ray intensities for the low and high temperature standards at every oxide thickness is expected to be less than 1 since the low temperature standard should have a lower density and therefore produces a weaker oxygen x-ray intensity. But from Fig. 7, this ratio varies from 0.93 to 1.12 in a somewhat random way and, therefore, suggests that the difference in the densities of the low temperature standard (synthesized at room temperature) and the high temperature standard (synthesized at 425 ºC) is much smaller than the instrumental/operational error bars associated with the data listed in Table 3 (or plotted in Figs. 5 & 6). This also implies that if an error bar on the order of 12% is acceptable, the calibration curves presented in Figs. 5 & 6 are also good for extracting thicknesses from samples with oxides grown in the temperature range of ~27 ºC to 425 ºC.”.

In another effort to crosscheck the accuracy of the presented EPMA technique against other means of oxide measurement, the thickness of a PuO_2 film grown on a Pu sample was probed by both ellipsometry [16] and EPMA calibration curve technique. The oxide measurements near the center of the sample yields 151 ± 2 nm and 166 ± 11 nm from ellipsometry and EPMA calibration curve method, respectively, for a difference of about 10%.

4. CONCLUSION

Oxygen content, humidity level, heat, and time are variables that can considerably affect the crystallinity, density, growth rate, and therefore thickness of PuO_2 films grown on Pu substrates. In this report, a cost-effective, non-destructive, and reliable method to determine the thickness of the oxides formed on Pu metal samples based on calibration curves has been described. As mentioned in the previous sections, a complimentary technique such as AES or XRD must be applied to confirm the PuO_2 nature of the samples and oxide standards. These calibration curves contain oxide thicknesses on Pu metal samples based on FIB trenching and cross-section SEM on the horizontal axis and EPMA oxygen k-ratios on the vertical axis. Oxide thickness measurements for the calibration curves were made on Pu metal samples within the typical SEM observable range for PuO_2 (35 – 400 nm). The portion of the calibration curve in the thinner oxide region (< 35 nm) were approximated via Pouchou and Pichoir's $\varphi(\rho z)$ theory. The use of PuO_2 standards offers a distinct advantage compared to other methods of thin film analysis because it provides the EPMA user with oxygen characteristic X-ray intensity values for the k-ratios from a known source synthesized by controlled growth conditions. The standards produce reliable oxygen X-ray intensities upon which the intensity values from the PuO_2 thin films can be used to calculate accurate k-ratio values and conclusive PuO_2 thicknesses. Even though cross-section SEM measurement was employed in this report to obtain the oxide thicknesses for the

calibration curves, other established techniques for thin film measurement such as ellipsometry, reflectivity, etc. can be considered as alternatives. This method, designed for the EPMA, will serve the plutonium research community as an effective tool for PuO_2 oxide thickness determination when other alternative methods are not available or impractical under certain circumstances. This method can also serve as a template for the creation of EPMA calibration curves for other actinide oxides that require film thickness measurements.

ACKNOWLEDGMENT

This work was performed under the auspices of the U.S. Department of Energy by Lawrence Livermore National Laboratory under Contract DE-AC52-07NA27344.

REFERENCES

[1] J. M. Haschke, J. C. Martz, Plutonium Storage, in: Encyclopedia of Environmental Analysis and Remediation, New York: John Wiley and Sons, Vol. 6, (1998) 3740.

[2] John M. Haschke, Thomas H. Allen, Joseph C. Martz, Oxidation kinetics of plutonium in air: consequences for environmental dispersal, Journal of Alloys and Compounds **271–273** (1998) 211–215.

[3] T. Nothwang, C. C. Davis, R. E. Lakis, Measuring the Thickness of Native Plutonium Oxides Using EPMA, *Microscopy and Microanalysis* **11** (2005) 1306-1307.

[4] D. R. Baer, M. H. Engelhard, A. S. Lea, P. Nachimuthu, T. C. Droubay, J. Kim, B. Lee, C. Mathews, R. L. Opila, L. V. Saraf, W. F. Stickle, R. M. Wallace, B. S. Wright, Comparison of the sputter rates of oxide films relative to the sputter rate of SiO_2, Journal of Vacuum Science & Technology **28** (2010) 1060.

[5] C. K. Saw, W. K. Grant, J. A. Stanford, L. N. Dinh, An Investigation on X-ray Reflectivity technique at LLNL, *LLNL-TR-680742* (2016).

[6] FEI Company: Quanta 3D FEG 200 / 600 User Operation Manual. 7th Edition. 11th November 2009.

[7] J. N. Hilfiker, R. A. Synowicki, H. G. Tompkins, Spectroscopic Ellipsometry for Thin Absorbing Films, 51st Annual Technical Conference Proceedings, Chicago, IL, April 19–24, 2008.

[8] JEOL XM-27470THIN Thin Film Analysis Instruction Manual

[9] M. Takakura, H. Takahashi, T. Okumura, Thin-film analysis with electron probe X-ray microanalyzer, *JEOL News* ***33E*** (1998) 15-19.

[10] J. I. Goldstein, D. E. Newbury, P. Echlin, D. C. Joy, A. D. Romig, C. E. Lyman, C. Fiori, E. Lifshin, *Scanning Electron Microscopy and X-ray Microanalysis*, 2nd ed., Plenum Press, New York (1992) 472-476.

[11] M. Matthews, B. Buse, S. L. Kearns, Electron Probe Microanalysis Through Coated Oxidized Surfaces, *Microscopy and Microanalysis* ***25*** (2019) 1112-1129.

[12] P. Willich, K. Schiffmann, EPMA of Surface Oxide Films, in: A. Boekestein & M. K. Pavicevic (Eds.), Electron Microbeam Analysis: Mikrochimica Acta Supplement, Vienna: Springer (1992) 221–227.

[13] Y. Osada, Electron Probe Microanalysis (EPMA) Measurement of Aluminum Oxide Film Thickness in the Nanometer Range on Aluminum Sheets. *X-ray Spectrometry* 34 (2004) 92-95.

[14] G. Auclair, C. Houpert, P. Chouquet, Determination by EPMA and X-ray Diffraction of the Thickness, Stoichiometry and Crystallinity of Thin Films (Cr_XO_Y) Deposited on Stainless Steels. *Inst. Phys. Conf.*, Ser. No 130, Chapter 2 (1992) 139-143.

[15] *STRATAGem 4.2 User's Manual; SAMx*

[16] L. N. Dinh, J. A. Stanford, C. K. Saw, A. J. Nelson, R. Gollott, J. M. Haschke, P. G. Allen, C. Gardner, C. Hrousis, W. J. Siekhaus, W. McLean II, Spectroscopic ellipsometry extraction of optical constants for materials from oxide covered samples: Application to the plutonium/oxides system. *Journal of Applied Physics* **125** (2019)183102.

[17] K. F. J. Heinrich, D. E. Newbury, (editors) *Electron Probe Quantitation*, 1st ed.; Springer Science + Business Media, LLC: New York (1991) 37-39.

[18] Casino software. http://www.gel.usherbrooke.ca/casino/ (accessed Feb 4, 2019).

[19] Practical Techniques for Microprobe Analysis; JEOL LTD.

[20] S. B. Donald, J. A. Stanford, A. J. Nelson, W. McLean II, Application of linear least squares to the analysis of Auger electron spectroscopy depth profiles of plutonium oxides. *Journal of Vacuum Science & Technology A* **36** (2018) 03E104.

[21] J. Goldstein, D. E. Newbury, D. C. Joy, C. E. Lyman, P. Echlin, E. Lifshin, L. Sawyer, J. R. Michael, *Scanning Electron Microscopy and X-ray Microanalysis*, 3rd ed.; Springer Science + Business Media, LLC: Boston (2003) 408.